

# Effect of Spherical Confinement on Chemical Reactivity

P. K. Chattaraj\* and U. Sarkar

Department of Chemistry, Indian Institute of Technology, Kharagpur 721302, India

Received: February 7, 2003; In Final Form: March 24, 2003

Numerical Hartree–Fock calculations have been performed with Dirichlet boundary conditions to calculate various global reactivity descriptors such as softness, electronegativity, polarizability, electrophilicity index, and mean excitation energy for several atoms (He, Li, Be, B, C, N, O, F, Ne) and ions ( $C^+$ ,  $C^{2+}$ ,  $C^{3+}$ ,  $C^{4+}$ ) confined in a spherical box. All of the systems become harder and less polarizable with a decrease in confinement volume. Electronegativity and electrophilicity are not very sensitive, except for very small cutoff radius at which they change abruptly. Mean excitation energy decreases with an increase in the box size. Linear relationship between softness and the cube-root of polarizability is observed for all of the confined atoms and ions. Scaled hardness shows opposite trends of softness, except for Li. Expected behavior is observed for the energy, virial, and various moments. With ionization, systems become more electronegative, harder, and less polarizable at all sizes.

## 1. Introduction

Confined quantum mechanical systems are useful models for simulating the effect of external conditions on an enclosed atom. The model of confined quantum systems has been used in many branches of physics, chemistry, and biology.<sup>1</sup> This model is used to study the effect of pressure on energy levels, polarizability of atoms and molecules, semiconductors, quantum dots,<sup>1</sup> matters under high pressure, and impurities or defects in crystal.<sup>1</sup> The physical properties of confined atoms and molecules depend on the confinement volume.<sup>2–7</sup> To our knowledge chemical reactivity parameters, softness ( $S$ ), hardness ( $\eta$ ), chemical potential ( $\mu$ ) (or electronegativity ( $\chi$ )), electrophilicity index ( $W$ ), etc., of many-electron systems under confinement have not been reported earlier. Here, we have calculated  $S$ ,  $\mu$ ,  $W$ , energy ( $E$ ), kinetic energy ( $T$ ), potential energy ( $V$ ), and moments ( $\langle r \rangle$ ,  $\langle 1/r \rangle$ , and  $\langle 1/r^2 \rangle$ ) for He, Li, Be, B, C, N, O, F, and Ne atoms and some ions ( $C^+$ ,  $C^{2+}$ ,  $C^{3+}$ , and  $C^{4+}$ ). Because the electron density vanishes at the confining radius,  $R_c$ , of a confined system, we have used Dirichlet's boundary condition.

In last few decades density functional theory (DFT)<sup>8</sup> has been applied to understand many problems in physics and chemistry. In DFT, the energy is a function of the electron density,  $\rho(\vec{r})$ ,

$$E[\rho(\vec{r})] = F[\rho(\vec{r})] + \int \rho(\vec{r})v(\vec{r}) d\vec{r} \quad (1)$$

where  $v(\vec{r})$  is the potential external to the electron cloud and  $F[\rho(\vec{r})]$  is the Hohenberg–Kohn universal functional<sup>8</sup> given, within a local density approximation for an atom, as

$$F[\rho] = C_k \int \rho^{(5/3)} d\vec{r} - \frac{1}{40} \int \frac{\vec{r} \cdot \nabla \rho}{r^2} d\vec{r} - C_x \int \rho^{(4/3)} d\vec{r} - \int \frac{\rho}{9.81 + 21.437\rho^{(-1/3)}} d\vec{r} + \frac{1}{2} \int \int \frac{\rho(\vec{r})\rho(\vec{r}')}{|\vec{r} - \vec{r}'|} d\vec{r} d\vec{r}' \quad (2)$$

where  $C_k = {}^{3/10}(3\pi^2)^{2/3}$  and  $C_x = ({}^{3/4})({}^{3/\pi})^{1/3}$ .

Chemical reactivity parameters such as electronegativity<sup>9</sup> ( $\chi$ ) and hardness<sup>10</sup> ( $\eta$ ) for an  $N$ -electron system with total energy  $E$  have been defined as

$$\chi = -\mu = -\left(\frac{\partial E}{\partial N}\right)_{v(\vec{r})} \quad (3)$$

and

$$\eta = \frac{1}{2} \left(\frac{\partial^2 E}{\partial N^2}\right)_{v(\vec{r})} = \frac{1}{2} \left(\frac{\partial \mu}{\partial N}\right)_{v(\vec{r})} \quad (4)$$

where  $\mu$  is the chemical potential.

An alternative definition of hardness<sup>11</sup> is

$$\eta = \frac{1}{N} \int \int \eta(\vec{r}, \vec{r}') f(\vec{r}') \rho(\vec{r}) d\vec{r} d\vec{r}' \quad (5)$$

where  $f(\vec{r})$  is the Fukui function<sup>12,13</sup> and  $\eta(\vec{r}, \vec{r}')$  is the hardness kernel. The Fukui function<sup>13</sup> and hardness kernels<sup>11</sup> are, respectively, given by

$$f(\vec{r}) = \left(\frac{\partial \rho(\vec{r})}{\partial N}\right)_{v(\vec{r})} = \left(\frac{\partial \mu}{\partial v(\vec{r})}\right)_N \quad (6)$$

and

$$\eta(\vec{r}, \vec{r}') = \frac{1}{2} \frac{\delta^2 F[\rho]}{\delta \rho(\vec{r}) \delta \rho(\vec{r}')} \quad (7)$$

Softness is the reciprocal of 2 times the hardness. Pearson<sup>14</sup> introduced the concept of hardness, which forms the basis of the hard–soft acid–base (HSAB)<sup>10,15,16</sup> principle stated as “hard acids like hard bases and soft acids like soft bases in an acid–base reaction”.

It has been proposed by Ghanty et al.<sup>17</sup> that scaled hardness is a better quantity to locate fixed points in the hardness profile, which is defined as

\* To whom correspondence should be addressed. E-mail: pkc@chem.iitkgp.ernet.in.

$$\eta_s = \frac{\eta}{|\mu|^{1/3}} \quad (8)$$

The many-electron system is completely characterized by  $N$  and  $\nu(\vec{r}')$ .

While  $\chi$  and  $\eta$  take care of the response of a system at constant  $\nu(\vec{r}')$  when  $N$  changes, the pertinent quantity in the opposite situation is the linear response function,<sup>8</sup>  $R(\vec{r}, \vec{r}')$ , which is the variation of density at a point  $\vec{r}$  under a change in the potential  $\nu(\vec{r}')$  keeping the total number of electrons ( $N$ ) constant, that is,

$$R(\vec{r}, \vec{r}') = \left( \frac{\delta \rho(\vec{r})}{\delta \nu(\vec{r}')} \right)_N \quad (9)$$

Within a density functional framework, this response function can be written<sup>8,11</sup> as

$$R(\vec{r}, \vec{r}') = \frac{s(\vec{r})s(\vec{r}')}{S} - s(\vec{r}, \vec{r}') \quad (10)$$

where  $s(\vec{r})$ ,  $S$ , and  $s(\vec{r}, \vec{r}')$  are the local softness, global softness ( $S = 1/(2\eta)$ ), and softness kernel, respectively.

The static electric dipole polarizability, which describes the response of the system when  $\nu(\vec{r}')$  changes at constant  $N$ , can be expressed in terms of the linear response function,  $R(\vec{r}, \vec{r}')$ , as follows<sup>8,18–20</sup>

$$\alpha = - \int \int R(\vec{r}, \vec{r}') \nu(\vec{r}) \nu(\vec{r}') d\vec{r} d\vec{r}' \quad (11)$$

Another useful quantity,  $I_o$ , the mean excitation energy, which describes the ability of a system to absorb energy, is the excitation energy weighted first moment of the dipole oscillator strength distribution defined using Bethe–Bloch<sup>21</sup> equation as<sup>22</sup>

$$I_o = 2\sqrt{\pi}\gamma \exp\left[\frac{-S_\rho}{2N}\right] \quad (12)$$

where  $N$  is the total number of electrons per atom and  $S_\rho$  is the Shannon entropy of the electron density,  $\rho(\vec{r})$ , and is given by

$$S_\rho = - \int \rho(\vec{r}) \ln \rho(\vec{r}) d\vec{r} \quad (13)$$

The constant  $\gamma$  ranges from 1 to  $\sqrt{2}$ .

The electrophilicity index<sup>23</sup> ( $W$ ), which measures the propensity to soak up electrons, is defined as

$$W = \frac{\mu^2}{2\eta} \quad (14)$$

In this paper, we have calculated several chemical reactivity parameters, such as  $S$ ,  $\alpha$ ,  $\chi$ ,  $\eta_s$ ,  $W$ ,  $I_o$  and various moments,  $\langle r^n \rangle$ , for several confined atoms and ions ( $C^+$ ,  $C^{2+}$ ,  $C^{3+}$ , and  $C^{4+}$ ). We have reported how these physico-chemical properties change because of the effect of confinement. Numerical details are given in section 2, and section 3 provides the results and discussion. Section 4 contains some concluding remarks.

## 2. Numerical Details

We have solved the nonrelativistic Hartree–Fock–Slater equation for atoms and ions using standard Herman–Skillman program<sup>24</sup> to obtain the self-consistent field (SCF) electronic wave function. The effect of confinement is incorporated via a Dirichlet boundary condition. This is done by multiplying the SCF wave function (before normalization and during each

iteration cycle) by a step function of the type  $\Theta = \exp[-r/R_c]^\lambda$ , where  $R_c$  is the cutoff radius and  $\lambda$  ( $=20$ ) is a parameter<sup>25</sup> that helps to vanish the wave function on the surface of the spherical box.<sup>25</sup> After the wave function or density is obtained from the Herman–Skillman program modified as above by Boeyens,<sup>25</sup> all reactivity parameters are calculated.

The hardness kernel,  $\eta(\vec{r}, \vec{r}')$ , as defined by Fuentealba<sup>19</sup> in local density model is given by

$$\eta(\vec{r}, \vec{r}') = \frac{\delta(\vec{r}, \vec{r}')}{2s(\vec{r})} \quad (15)$$

where  $s(\vec{r})$  is the local softness. The integration of  $s(\vec{r})$  over whole space gives global softness,<sup>19,20</sup>  $S$ ,

$$S = \int s(\vec{r}) d\vec{r} \quad (16)$$

The relation between global softness and global hardness is given by

$$\eta = \frac{1}{2S} \quad (17)$$

The scaled hardness is calculated using eq 8.

The chemical potentials have been calculated by equating the chemical potential with the total electrostatic potential at a point  $\vec{r}_c$ <sup>26</sup> where the sum of the functional derivatives of kinetic energy and exchange–correlation energy with respect to  $\rho(\vec{r})$  is zero, that is,

$$\mu = -\chi = -\frac{Z}{r_c} + \int \frac{\rho(\vec{r})}{|\vec{r} - \vec{r}_c|} d\vec{r} \quad (18)$$

The static dipole polarizabilities<sup>19,20</sup> ( $\alpha$ ) have been calculated using local softness  $s(\vec{r})$  as follows:

$$\alpha = \frac{4\pi}{3} \int_0^\infty s(r)r^4 dr \quad (19)$$

Note that this equation is valid for spherically averaged density.

We have calculated mean excitation energy using eq 12 with a  $\gamma$  value of 1.0107. We have taken this  $\gamma$  value to reproduce the numerical Hartree–Fock  $I_o$  value<sup>22</sup> (35.39 eV) for He atom.

## 3. Results and Discussion

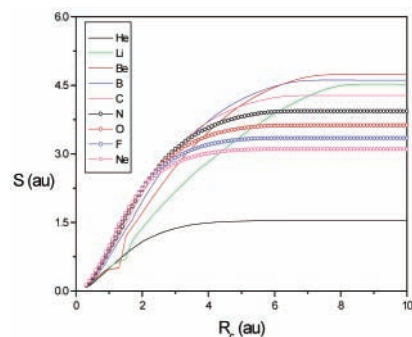
Table 1 presents the moments,  $\langle r \rangle$ ,  $\langle 1/r \rangle$ , and  $\langle 1/r^2 \rangle$ , the total energy, and the virial at some selected cutoff radii of different confined atoms (He, Li, Be, B, C, N, O, F, and Ne) and ions ( $C^+$ ,  $C^{2+}$ ,  $C^{3+}$ , and  $C^{4+}$ ). Energy and its components are calculated using near-Hartree–Fock density in eq 1. The energy values and virial are highly satisfactory, and different expectation values follow similar trends<sup>2</sup> as was obtained in a variation perturbation calculation.<sup>27</sup> Virial remains very close to 2 except for the cases in which the spherical box becomes very small, so that the total energy becomes positive in most cases.

Figure 1 presents the variation of global softness with respect to cutoff radius,  $R_c$ , for all of the atoms studied here, and Figure 2 presents the same for ions ( $C^+$ ,  $C^{2+}$ ,  $C^{3+}$ , and  $C^{4+}$ ). The softness values match well with those reported in the literature.<sup>19</sup> From the figures, it is clear that the system becomes harder with a rapid change for small radius values. Various elements exhibit expected softness trends, and a system becomes gradually harder with degree of ionization. The He and Ne atoms are the hardest among the systems studied, as expected from the maximum hardness principle<sup>28</sup> in relation to the extra stability of these atoms due to closed-shell structure.<sup>29</sup>

**TABLE 1: Effect of Spherical Confinement on  $\langle r \rangle$  (au),  $\langle 1/r \rangle$  (au), Total Energy (au), and the Virial for Different Atoms and Ions**

atom	$R_c$	$\langle r \rangle$	$\langle 1/r \rangle$	$\langle 1/r^2 \rangle$	$-E$	$-V/T$
He	10.0	0.940 246	1.692 418	6.106 651	2.9060	2.0846
	7.5	0.940 244	1.692 419	6.106 653	2.9060	2.0846
	5.0	0.939 570	1.692 581	6.107 062	2.9059	2.0844
	3.0	0.917 871	1.701 663	6.134 809	2.8990	2.0706
	0.5	0.322 806	3.728 090	21.534 200	-4.9521	0.7044
Li	10.0	1.470 891	1.962 774	10.635 146	7.5114	1.9991
	7.5	1.508 589	1.965 956	10.634 295	7.5256	2.0090
	5.0	1.384 117	1.984 263	10.674 897	7.5334	2.0029
	3.0	1.089 061	2.038 449	10.833 226	7.5447	1.9769
	0.5	0.300 947	4.140 569	27.723 220	-9.4724	0.7470
Be	10.0	1.481 473	2.150 253	14.968 291	14.8381	2.0240
	7.5	1.487 557	2.150 816	14.967 692	14.8437	2.0269
	5.0	1.426 802	2.158 502	14.986 333	14.8487	2.0247
	3.0	1.186 060	2.203 420	15.108 205	14.8773	2.0062
	0.5	0.278 170	4.640 952	36.149 510	-16.7110	0.7662
B	10.0	1.330 416	2.323 609	19.300 097	25.2022	2.0450
	7.5	1.333 229	2.323 910	19.299 500	25.2069	2.0468
	5.0	1.303 571	2.327 073	19.300 643	25.2115	2.0473
	3.0	1.156 508	2.352 052	19.317 188	25.2285	2.0394
	0.5	0.250 413	5.582 754	59.212 714	-35.2559	0.7459
C	10.0	1.170 825	2.495 976	23.682 132	38.8883	2.0575
	7.5	1.171 339	2.496 065	23.681 985	38.8900	2.0580
	5.0	1.158 428	2.497 415	23.681 056	38.8924	2.0585
	3.0	1.074 995	2.511 158	23.663 526	38.8864	2.0547
	0.5	0.258 322	5.735 142	67.641 115	-38.0432	0.8021
N	10.0	1.036 438	2.666 657	28.130 032	56.0868	2.0588
	7.5	1.036 481	2.666 703	28.129 944	56.0874	2.0589
	5.0	1.031 159	2.667 284	28.129 353	56.0884	2.0592
	3.0	0.982 980	2.676 070	28.115 671	56.0600	2.0564
	0.5	0.278 250	5.513 642	68.334 864	-23.2055	0.8974
O	10.0	0.927 735	2.836 110	32.651 829	76.9395	2.0505
	7.5	0.927 722	2.836 125	32.651 811	76.9397	2.0505
	5.0	0.925 527	2.836 379	32.651 384	76.9403	2.0507
	3.0	0.897 123	2.842 507	32.648 249	76.8962	2.0483
	0.5	0.295 855	5.177 581	64.670 471	-1.0965	0.9956
F	10.0	0.839 344	3.004 251	37.246 775	101.5363	2.0347
	7.5	0.839 344	3.004 253	37.246 775	101.5363	2.0347
	5.0	0.838 415	3.004 372	37.246 510	101.5367	2.0348
	3.0	0.821 547	3.008 562	37.247 458	101.4878	2.0331
	0.5	0.304 814	4.958 787	62.058 301	18.9101	1.0675
Ne	10.0	0.766 285	3.171 599	41.917 802	129.9199	2.0130
	7.5	0.766 284	3.171 599	41.917 802	129.9199	2.0130
	5.0	0.765 898	3.171 656	41.917 667	129.9202	2.0130
	3.0	0.755 831	3.174 471	41.919 440	129.8731	2.0118
	0.5	0.307 565	4.868 139	61.728 877	37.8298	1.1174
C <sup>+</sup>	10.0	0.975 914	2.876 678	28.460 709	38.5940	2.0659
	7.5	0.975 914	2.876 681	28.460 704	38.5940	2.0659
	5.0	0.973 942	2.876 973	28.461 046	38.5951	2.0658
	3.0	0.935 918	2.885 814	28.470 446	38.628	2.0643
	0.5	0.235 627	6.298 744	79.126 041	-23.1758	0.8662
C <sup>2+</sup>	10.0	0.810 548	3.404 117	35.612 962	37.5237	2.0575
	7.5	0.810 547	3.404 117	35.612 963	37.5237	2.0575
	5.0	0.810 321	3.404 165	35.613 175	37.5239	2.0575
	3.0	0.794 857	3.408 942	35.630 499	37.5503	2.0570
	0.5	0.222 306	6.316 709	71.118 433	1.8921	1.0152
C <sup>3+</sup>	10.0	0.597 864	4.216 384	46.283 268	35.7695	2.0570
	7.5	0.597 864	4.216 384	46.283 268	35.7695	2.0570
	5.0	0.597 834	4.216 392	46.283 307	35.7695	2.0570
	3.0	0.592 394	4.218 610	46.294 173	35.7834	2.0569
	0.5	0.216 947	6.527 435	81.098 445	22.6154	1.2771
C <sup>4+</sup>	10.0	0.267 759	5.690 170	65.555 057	32.9366	2.0563
	7.5	0.267 759	5.690 170	65.555 057	32.9366	2.0563
	5.0	0.267 759	5.690 170	65.555 057	32.9366	2.0563
	3.0	0.267 759	5.690 170	65.555 057	32.9366	2.0563
	0.5	0.229 410	6.128 826	72.168 468	32.0207	1.8696

Figures 3 and 4 illustrate how polarizability is changing with the change of cutoff radius,  $R_c$ , for the atoms and ions,



**Figure 1.** Plot of softness ( $S$ , au) versus cutoff radius ( $R_c$ , au) for atoms confined in a spherical box: (black  $\rightarrow$ ) He; (green  $\rightarrow$ ) Li; (red  $\rightarrow$ ) Be; (blue  $\rightarrow$ ) B; (pink  $\rightarrow$ ) C; (black  $\circ$ ) N; (red  $\circ$ ) O; (blue  $\circ$ ) F; (pink  $\circ$ ) Ne.

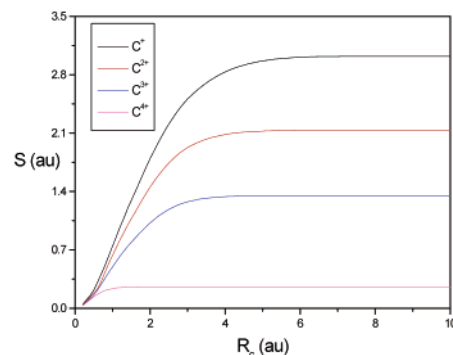


**Figure 2.** Plot of softness ( $S$ , au) versus cutoff radius ( $R_c$ , au) for ions confined in a spherical box: (black  $\rightarrow$ ) C<sup>+</sup>; (red  $\rightarrow$ ) C<sup>2+</sup>; (blue  $\rightarrow$ ) C<sup>3+</sup>; (pink  $\rightarrow$ ) C<sup>4+</sup>.

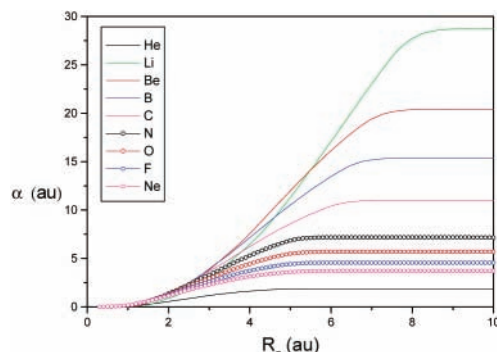


**Figure 3.** Plot of polarizability ( $\alpha$ , au) versus cutoff radius ( $R_c$ , au) for atoms confined in a spherical box: (black  $\rightarrow$ ) He; (green  $\rightarrow$ ) Li; (red  $\rightarrow$ ) Be; (blue  $\rightarrow$ ) B; (pink  $\rightarrow$ ) C; (black  $\circ$ ) N; (red  $\circ$ ) O; (blue  $\circ$ ) F; (pink  $\circ$ ) Ne.

respectively. With the decrease of the confinement radius, the polarizability decreases monotonically and approaches zero for very small radius. For the systems considered in the present work, the He and Ne atoms are least polarizable because of their closed-shell structure,<sup>29</sup> which is in conformity with the minimum polarizability principle.<sup>30</sup> On ionization, a system becomes more difficult to polarize.

The inverse relationship between  $S$  and  $\alpha^{(1/3)}$  is clearly manifested in Figures 5 and 6 for atoms and ions, respectively. Many researchers have shown<sup>31</sup> the linear behavior of  $S$  as a function of  $\alpha^{(1/3)}$  for atoms, molecules, and clusters. But this behavior is clearly delineated by the respective regression coefficients (shown along with the individual curves) and is shown here for the first time for the confined systems.

The behavior of mean excitation energy ( $I_0$ ) as a function of confinement for atoms and ions is depicted, respectively, in

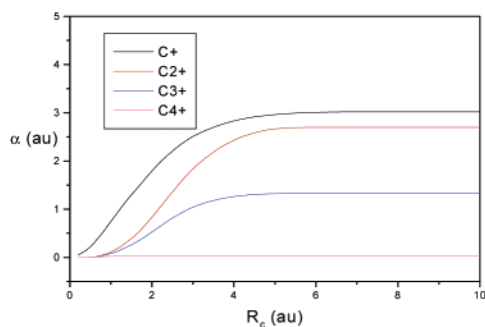


**Figure 4.** Plot of polarizability ( $\alpha$ , au) versus cutoff radius ( $R_c$ , au) for ions confined in a spherical box: (black —)  $C^+$ ; (red —)  $C^{2+}$ ; (blue —)  $C^{3+}$ ; (pink —)  $C^{4+}$ .

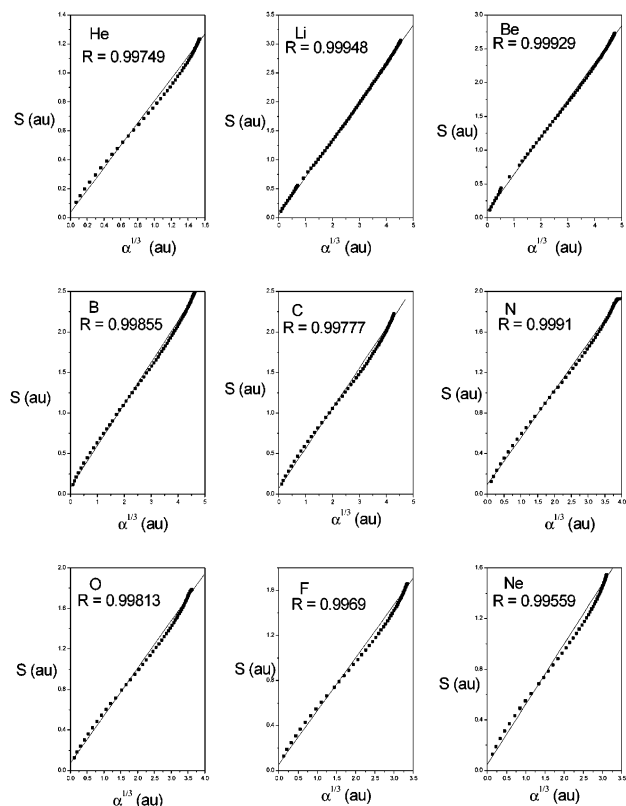


**Figure 5.** Plot of softness ( $S$ , au) versus  $\alpha^{1/3}$  (au) for atoms confined in a spherical box.

Figures 7 and 8. The energy values for large  $R_c$  are in good agreement with those reported by Hó et al.<sup>22</sup> Note that the qualitative behavior of our figures is the same as that obtained by Sabin and Sabin.<sup>32</sup>

Figures 9 and 10 graphically illustrate the behavior of electronegativity as a function of  $R_c$  for all of the atoms and ions, respectively. We have seen from the figures that  $\chi$  is not very sensitive to confinement, except for a very small  $R_c$  at which it shoots up to a high value. Among the atoms studied, the large electronegativity of F and small electronegativity of Li conform to chemical intuition, and the overall trend is similar to that reported in literature.<sup>33</sup> As expected,  $\chi$  increases in the order  $C^+ < C^{2+} < C^{3+} < C^{4+}$ .

In Figures 11 and 12, we have presented the effect of confinement on scaled hardness. From Figure 11, it is obvious that fluorine has highest  $\eta_s$  value, while lithium has the lowest one, and for ions (see Figure 12),  $C^{4+}$  has the highest and  $C^+$  has the lowest value. The behavior of the two graphs are also

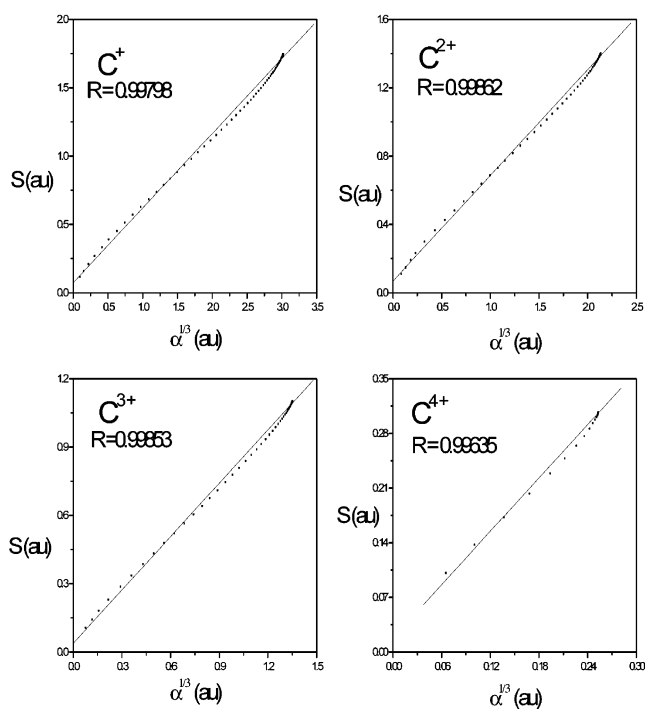


**Figure 6.** Plot of softness ( $S$ , au) versus  $\alpha^{1/3}$  (au) for ions confined in a spherical box.

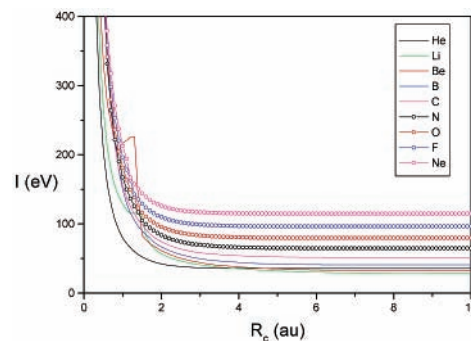


**Figure 7.** Plot of mean excitation energy ( $I_0$ , eV) versus cutoff radius ( $R_c$ , au) for atoms confined in a spherical box: (black —) He; (green —) Li; (red —) Be; (blue —) B; (pink —) C; (black ○) N; (red ○) O; (blue ○) F; (pink ○) Ne.

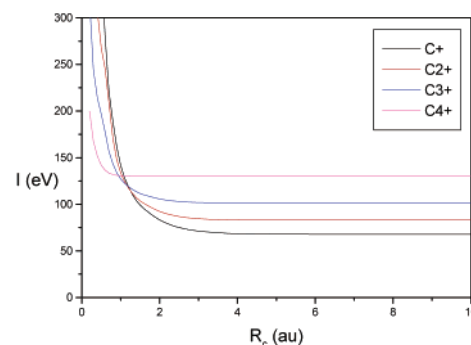


**Figure 8.** Plot of mean excitation energy ( $I_0$ , eV) versus cutoff radius ( $R_c$ , au) for ions confined in a spherical box: (black —)  $C^+$ ; (red —)  $C^{2+}$ ; (blue —)  $C^{3+}$ ; (pink —)  $C^{4+}$ .

similar. These plots are in conformity with the corresponding softness plots.

The electrophilicity index ( $W$ ) is presented in Figures 13 and 14 for atoms and ions, respectively. It is seen that  $W$  is not very sensitive to confinement except for very small  $R_c$  values.



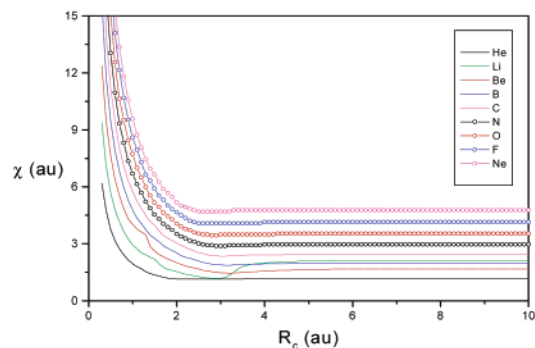


**Figure 9.** Plot of electronegativity ( $\chi$ , au) versus cutoff radius ( $R_c$ , au) for atoms confined in a spherical box: (black  $\rightarrow$ ) He; (green  $\rightarrow$ ) Li; (red  $\rightarrow$ ) Be; (blue  $\rightarrow$ ) B; (pink  $\rightarrow$ ) C; (black  $\circ$ ) N; (red  $\circ$ ) O; (blue  $\circ$ ) F; (pink  $\circ$ ) Ne.

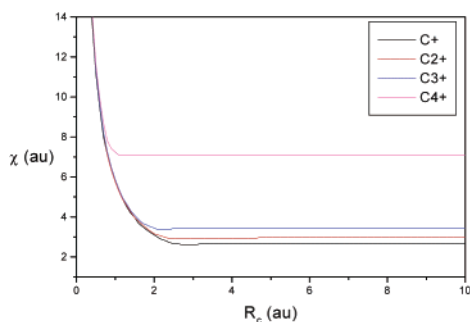


**Figure 10.** Plot of electronegativity ( $\chi$ , au) versus cutoff radius ( $R_c$ , au) for ions confined in a spherical box: (black  $\rightarrow$ ) C<sup>+</sup>; (red  $\rightarrow$ ) C<sup>2+</sup>; (blue  $\rightarrow$ ) C<sup>3+</sup>; (pink  $\rightarrow$ ) C<sup>4+</sup>.

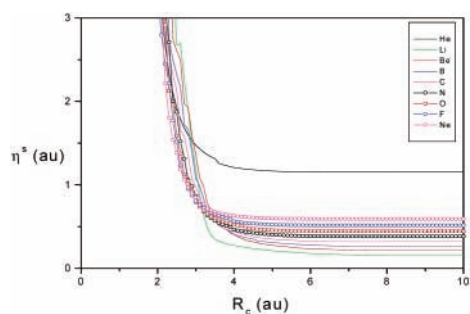


**Figure 11.** Plot of scaled hardness ( $\eta_s$ , au) versus cutoff radius ( $R_c$ , au) for atoms confined in a spherical box: (black  $\rightarrow$ ) He; (green  $\rightarrow$ ) Li; (red  $\rightarrow$ ) Be; (blue  $\rightarrow$ ) B; (pink  $\rightarrow$ ) C; (black  $\circ$ ) N; (red  $\circ$ ) O; (blue  $\circ$ ) F; (pink  $\circ$ ) Ne.

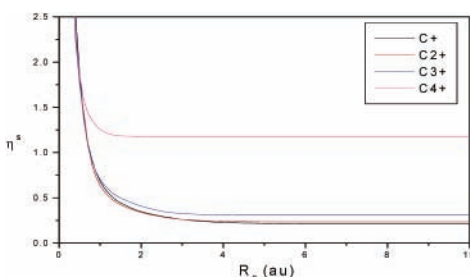


**Figure 12.** Plot of scaled hardness ( $\eta_s$ , au) versus cutoff radius ( $R_c$ , au) for ions confined in a spherical box: (black  $\rightarrow$ ) C<sup>+</sup>; (red  $\rightarrow$ ) C<sup>2+</sup>; (blue  $\rightarrow$ ) C<sup>3+</sup>; (pink  $\rightarrow$ ) C<sup>4+</sup>.

The relative electrophilicity of atoms and ions follows the same trend as that of electronegativity, as expected.

In Figures 15 and 16, we present the variation of kinetic energy, potential energy, and total energy as a function of  $R_c$  for atoms and ions, respectively. Kinetic energy becomes more

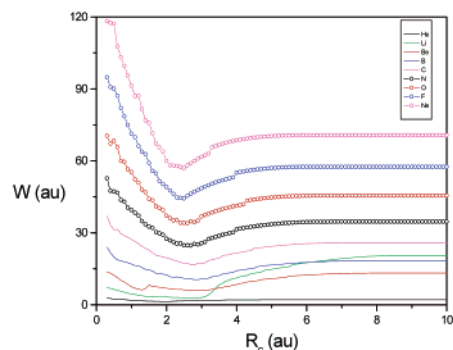


**Figure 13.** Plot of electrophilicity index ( $W$ , au) versus cutoff radius ( $R_c$ , au) for atoms confined in a spherical box: (black  $\rightarrow$ ) He; (green  $\rightarrow$ ) Li; (red  $\rightarrow$ ) Be; (blue  $\rightarrow$ ) B; (pink  $\rightarrow$ ) C; (black  $\circ$ ) N; (red  $\circ$ ) O; (blue  $\circ$ ) F; (pink  $\circ$ ) Ne.

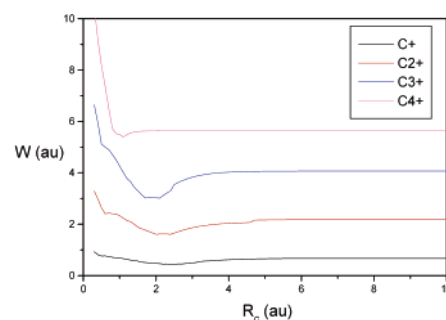


**Figure 14.** Plot of electrophilicity index ( $W$ , au) versus cutoff radius ( $R_c$ , au) for ions confined in a spherical box: (black  $\rightarrow$ ) C<sup>+</sup>; (red  $\rightarrow$ ) C<sup>2+</sup>; (blue  $\rightarrow$ ) C<sup>3+</sup>; (pink  $\rightarrow$ ) C<sup>4+</sup>.

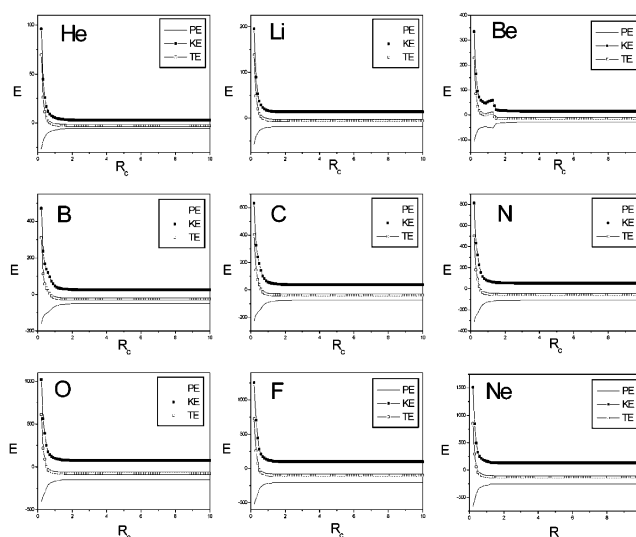


**Figure 15.** Plot of energy ( $E$ , au) versus cutoff radius ( $R_c$ , au) for atoms confined in a spherical box: ( $\rightarrow$ ) potential energy, ( $\blacksquare$ ) kinetic energy, and ( $\square$ ) total energy.

positive while potential energy becomes more negative as we decrease  $R_c$ . Note that the total energy becomes positive for very small  $R_c$ . Variation of the eigenvalues with the pressure is also an important aspect to be studied. A small portion of the present work has appeared elsewhere.<sup>34</sup>

#### 4. Concluding Remarks

Different global reactivity descriptors, softness, polarizability, electronegativity, electrophilicity index, mean excitation energy, etc., for several atoms and ions confined in a spherical box have been calculated using a self-consistent-field technique with

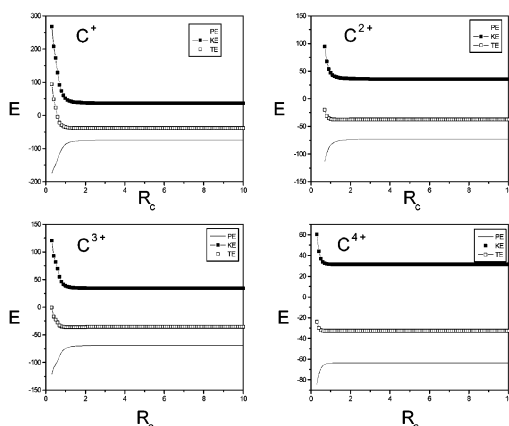


**Figure 16.** Plot of energy ( $E$ , au) versus cutoff radius ( $R_c$ , au) for ions confined in a spherical box: (—) potential energy, (■) kinetic energy, and (□) total energy.

proper boundary conditions. As we keep on decreasing the size of the spherical box, the system gets harder and less polarizable and becomes more difficult to excite. Scaled hardness mirrors the softness behavior, except for Li. For a given system, it becomes less electronegative, softer, and more polarizable at all cutoff radii values with an increase in the number of electrons with no change in the atomic number. Softness varies linearly with the cube root of polarizability for all of the confined atoms and ions.

**Acknowledgment.** We thank CSIR, New Delhi for financial assistance, reviewers for their constructive criticism, and Professor J. C. A. Boeyens for providing the necessary numerical code.

## References and Notes

- (1) (a) Jaskólski, W. *Phys. Rep.* **1996**, *271*, 1. (b) Michels, A.; Boer, J. D.; (c) Biji, A. *Physica* **1937**, *4*, 981. (d) Sommerfeld, A. *Ann. Phys.* **1938**, *32*, 56. (e) Groot, S. R. D.; Seldam, C. A. T. *Physica* **1946**, *12*, 669. (f) Buchachenko, A. L. *J. Phys. Chem. B* **2001**, *105*, 5839. (g) Banerjee, A.; Sen, K. D.; Garza, J.; Vargas, J. *J. Chem. Phys.* **2002**, *116*, 4054. (h) Gray, B. F.; Gonda, I. *J. Theor. Biol.* **1975**, *49*, 493. (i) Garza, J.; Vargas, R. Vela, A.; Sen, K. D.; *J. Mol. Struct. (THEOCHEM)* **2000**, *501–502*, 183. (j) Sen, K. D.; Garza, J.; Vargas, R.; Aquino, N. *Phys. Lett. A* **2002**, *295*, 299.
- (2) Ludeña, E. V. *J. Chem. Phys.* **1978**, *69*, 1770.
- (3) Ludeña, E. V.; Gregori, M. *J. Chem. Phys.* **1979**, *71*, 2235.
- (4) Gorecki, J.; Brown, B. W. *J. Phys. B: At. Mol. Phys.* **1988**, *21*, 403.

- (5) Marin, J. L.; Cruz, S. A. *J. Phys. B: At. Mol. Phys.* **1992**, *25*, 4365.
- (6) Marin, J. L.; Rosas, R.; Uribe, A. *Am. J. Phys.* **1995**, *63*, 460.
- (7) Corella-Mandueno, A.; Rosas, R.; Marin, J. L.; Riera, R. *Phys. Low-Dimens. Struct.* **1999**, *5/6*, 75.
- (8) Parr, R. G.; Yang, W. *Density Functional Theory of Atoms and Molecules*; Oxford University Press: New York, 1989.
- (9) Parr, R. G.; Donnelly, D. A.; Levy, M.; Palke, W. E. *J. Chem. Phys.* **1978**, *68*, 3801.
- (10) Parr, R. G.; Pearson, R. G. *J. Am. Chem. Soc.* **1983**, *105*, 7512.
- (11) (a) Berkowitz, M.; Ghosh, S. K.; Parr, R. G. *J. Am. Chem. Soc.* **1985**, *107*, 6811. (b) Ghosh, S. K.; Berkowitz, M. *J. Chem. Phys.* **1985**, *83*, 2976.
- (12) Fukui, K. *Theory of Orientation and Stereoselection*; Springer-Verlag: Berlin, 1973; p 134; *Science (Washington, D. C.)* **1982**, *218*, 747.
- (13) Parr, R. G.; Yang, W. *J. Am. Chem. Soc.* **1984**, *106*, 4049.
- (14) Pearson, R. G. *Coord. Chem. Rev.* **1990**, *100*, 403. *Hard and Soft Acids and Bases*; Dowden, Hutchinson and Ross: Stroudsburg, PA, 1973.
- (15) Pearson, R. G. *Chemical Hardness: Applications from Molecules to Solids*; Wiley-VCH Verlag GmbH: Weinheim, Germany, 1997.
- (16) Chattaraj, P. K.; Lee, H.; Parr, R. G. *J. Am. Chem. Soc.* **1991**, *113*, 1855.
- (17) Ghanty, T. K.; Ghosh, S. K. *J. Phys. Chem. A* **2002**, *106*, 4200.
- (18) Miller, T. M.; Bederson, B. *Adv. At. Mol. Phys.* **1977**, *13*, 1.
- (19) Fuentealba, P. *J. Chem. Phys.* **1995**, *103*, 6571.
- (20) Garza, J.; Robles, J. *Phys. Rev. A* **1993**, *47*, 2680.
- (21) Ahlen, S. P. *Rev. Mod. Phys.* **1980**, *52*, 121.
- (22) Hó, M.; Weaver, D. F.; Smith, V. H., Jr.; Sagar, P. R.; Esquivel, R. O. *Phys. Rev. A* **1998**, *57*, 4512.
- (23) Parr, R. G.; Szentpaly, L. v.; Liu, S. *J. Am. Chem. Soc.* **1999**, *121*, 1922.
- (24) Herman, F.; Skillman, S. *Atomic Structure Calculations*; Prentice-Hall; Englewood Cliffs, NJ, 1963.
- (25) Boeyens, J. C. A. *J. Chem. Soc., Faraday Trans.* **1994**, *90*, 3377.
- (26) Ludena, E. V. *J. Chem. Phys.* **1983**, *79*, 6174. Kryachko, E. S.; Ludena, E. V. *Density Functional Theory of Many-Electron Systems*; Kluwer: Dordrecht, Netherlands, 1990.
- (27) Gimarc, B. M. *J. Chem. Phys.* **1967**, *47*, 5110.
- (28) (a) Pearson, R. G. *J. Chem. Educ.* **1987**, *64*, 561. Pearson, R. G. *Acc. Chem. Res.* **1993**, *26*, 250. (b) Parr, R. G.; Chattaraj, P. K. *J. Am. Chem. Soc.* **1991**, *113*, 1854. (c) Pearson, R. G. *Chemtracts: Inorg. Chem.* **1991**, *3*, 317. (d) Ayers, P. W.; Parr, R. G. *J. Am. Chem. Soc.* **2000**, *122*, 2010. (e) Chattaraj, P. K. *Proc. Indian Natl. Sci. Acad., Part A* **1996**, *62*, 513.
- (29) Chattaraj, P. K.; Maiti, B. *J. Chem. Educ.* **2001**, *78*, 811.
- (30) Chattaraj, P. K.; Sengupta, S. *J. Phys. Chem.* **1996**, *100*, 16126.
- (31) Pearson, R. G. In *Chemical Hardness, Structure and Bonding*; Sen, K. D., Mingos, D. M. P., Eds.; Springer-Verlag: Berlin, 1993; Vol. 80. Politzer, P. *J. Chem. Phys.* **1987**, *86*, 1072. Ghanty, T. K.; Ghosh, S. K. *J. Phys. Chem.* **1993**, *97*, 4951. Fuentealba, P.; Reyes, O. *J. Mol. Struct. (THEOCHEM)* **1993**, *282*, 65. Fuentealba, P.; Simón-Manso, Y. *J. Phys. Chem. A* **1998**, *102*, 2029.
- (32) Sabin, P. B.; Sabin, J. R. *Int. J. Quantum Chem.* **2001**, *82*, 227.
- (33) Goycoolea, C.; Barrera, M.; Zuloaga, F. *Int. J. Quantum Chem.* **1989**, *36*, 455.
- (34) Chattaraj, P. K.; Sarkar, U. *Chem. Phys. Lett.* **2003**, *372*, 805.